Article

Seismic Performance of a 1:4 Scale Two-Story Rammed Earth Model Reinforced with Steel Plates Tested on a Bi-Axial Shaking Table

Natalia Barrera [1], Daniel M. Ruiz [1,*], Juan C. Reyes [2], Yezid A. Alvarado [1] and Daniela Carrasco-Beltrán [3]

1   Department of Civil Engineering, Pontificia Universidad Javeriana, Bogotá 110231, Colombia; natalia.barrera@javeriana.edu.co (N.B.); alvarado.y@javeriana.edu.co (Y.A.A.)
2   Department of Civil and Environmental Engineering, Universidad de los Andes, Bogotá 111711, Colombia; jureyes@uniandes.edu.co
3   Department of Architecture, Pontificia Universidad Javeriana, Bogotá 110231, Colombia; carrascod@javeriana.edu.co
*   Correspondence: daniel.ruiz@javeriana.edu.co

Abstract: During the 16th and 17th centuries, Latin American cities adopted earthen construction techniques from European colonizers. As a result, rammed earth (RE) buildings now occupy an important place in Latin America's cultural heritage. However, earthquakes around the world have shown that unreinforced earthen constructions are highly vulnerable. For several years, researchers in northern South America have been proposing a technique that consists of installing confining steel plates (or wooden elements) on both sides of the RE walls to form a grid. This system has shown excellent performance in controlling seismic damage and increasing strength and ductility capacity. Although researchers have tested full-scale one- and two-story earthen walls under pseudo-static loading in the laboratory, and one- and two-story earthen walls at 1:1 and 1:2 scales on uniaxial and biaxial shaking tables, the behavior of a complete reinforced module (one- or two-story) on a shaking table has never been assessed. The present study presents the results of shaking table tests performed on two-story RE modules at 1:4 scale. The experimental data indicate that the retrofit system with confining steel plates was effective in reducing the seismic damage of earthen constructions. In addition, the comparison of the results of the 1:4 scale tests with the 1:2 and 1:1 scale tests previously conducted by the researchers shows that the acceleration levels of the equivalent prototypes are in the same order of magnitude for the three scales.

Keywords: seismic retrofit; steel plates; earthen historic buildings; shaking table tests

1. Introduction

Earthen construction techniques have a rich and extensive history, dating back to the Neolithic period when humans first settled and began constructing permanent structures [1]. Throughout history, civilizations such as the Sumerians, Egyptians, and Babylonians, among others, have used various forms of earthen structures for dwellings, temples, and government buildings [2]. Today, earthen buildings serve as homes for at least 33% of the world's population and make up one-tenth of World Heritage Monuments [3]. For instance, in regions influenced by European colonial architecture, such as Colombia (northern South America), rammed earth (RE) buildings hold immense cultural value and most of them are considered heritage constructions [4]. The preservation of these architectural legacies becomes crucial, not only to maintain their cultural significance for future generations, but also because today, earthen buildings represent an ideal sustainable construction system due to their recyclability, and their low energy and water footprints. However, the deterioration of earthen buildings has accelerated due to natural and human impacts, including earthquakes, urbanization, and the adoption of industrialized building technologies [5].

Seismic performance has been a particular concern for unreinforced RE constructions due to their deficient structural behavior during past earthquakes. Events such as the Peru 2007 and the Chile 2010 earthquakes highlighted the vulnerability of historic earthen buildings to seismic forces [6,7]. The deficiencies in their seismic behavior can be attributed to factors such as poor material properties, irregular distribution of walls and openings, weak connections between walls, inadequate wall–floor–roof connections, heavy roofs and floors, and deficient out-of-plane strength [8–14]. Earthen buildings have evidenced partial collapse for 0.5% of inter-story drift levels [8,13,15]. For this reason, in the last four decades, there has been a growing motivation to improve the seismic performance of earthen buildings (RE and adobe), driven by the need for conservation of historical sites built with sustainable construction practices. Researchers worldwide have made significant efforts to develop retrofitting techniques for existing RE buildings. Various countries, including Peru [16], Australia [17], Germany [18], and more recently, Colombia [19], have established regulations and guidelines for seismic rehabilitation of earthen structures. The current rehabilitation techniques include bonded fibers, mesh reinforcement, tensors, polyester fabric strips, straps, steel cables, concrete beams, mortar with textiles, and confining elements (wood and steel plates) [6–9,12–15,20–29].

Among the retrofitting techniques proposed in the literature, confinement with wooden elements or steel plates have emerged as a prominent alternative for restoration purposes in order to preserve heritage building in the long term [4,8,9,15,21,28]. These reinforcements have demonstrated outstanding results in improving the overall capacities and seismic behavior of earthen walls in comparison to other rehabilitation techniques; for instance, the maximum residual drift is at least three times lower than the classic mesh reinforcement technique [8], ensuring the integrity of the building after large earthquakes. Both approaches (confinement with wooden elements or with steel plates) involve installing vertical and horizontal reinforcement elements approximately (each 1000 mm) on the inner and outer faces of the wall and interconnected with steel rods (each 500 mm). However, the reinforcement with wooden elements has significant drawbacks due to the large section of the strips (180 mm × 40 mm) and the durability issues of the material. To address these challenges, the use of steel plate confinement has gained attention in northern South America, as it offers advantages such as equal or superior efficiency compared to wooden elements, improved durability against external agents, less invasive installation, and smaller reinforcement element size (100 mm × 6.35 mm). Figure 1a shows a typical façade of an Andean historic earthen house, and Figure 1b allows a visualization of the wall with the reinforcement based on steel plates. In addition, the connection and compatibility between the two materials (rammed earth and steel plates) is provided by 9.5 mm diameter pass-through rods/bars placed every 500 mm. These bars are then welded (or sometimes bolted) to the steel plates. These connectors are made of steel with a minimum yield strength of 420 MPa, and Figure 1c shows an example of the installation. It is very important to note that once the steel plates are installed on both sides of the walls, they are covered with a layer of earth, lime, and sand so that the aesthetic of the building is not affected by the seismic reinforcement.

Despite the progress in this retrofit technique—with research projects including full-scale pseudo-static tests (one- and two-story earthen walls) and one- and two-story earthen wall tests on uniaxial and biaxial shake tables (1:1 and 1:2 scale)—there is a notable lack of studies concerning multi-story earthen houses (with interconnected walls) reinforced with steel plate confinement. The importance of this study arises from the prevalence of multi-story earthen heritage buildings throughout the world. For instance, in the case of the historic center of Bogota (the main city of Colombia, South America), which is one of the areas with the highest density of earthen buildings per square meter in the country, it has been reported that nearly 50% of the earthen historic constructions have two stories [30]. Therefore, this research aims to contribute to the understanding of the seismic behavior of earthen historic structures reinforced with steel plates in order to preserve the cultural heritage and promote sustainable construction buildings.
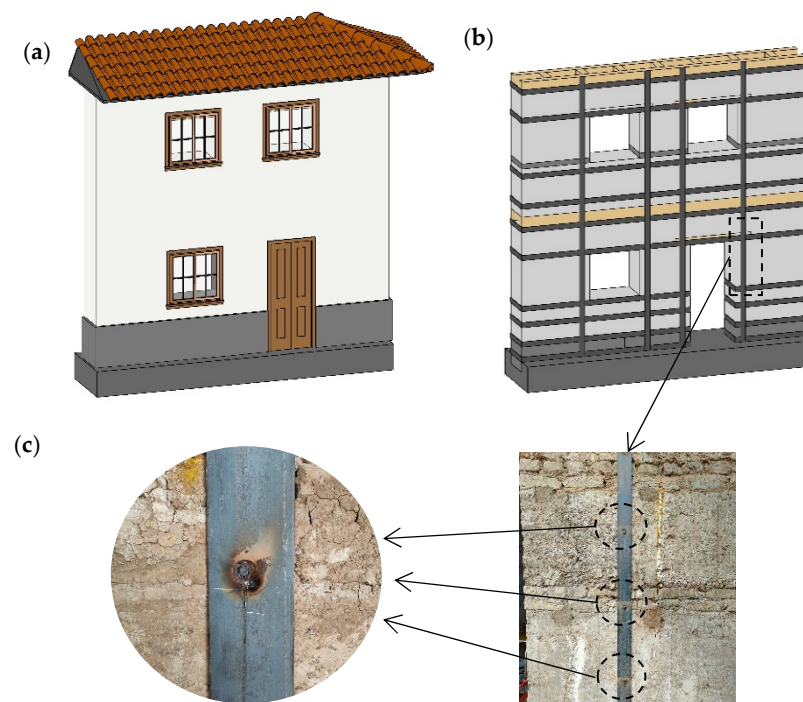
Figure 1. (**a**) Typical façade of an Andean heritage earthen house; (**b**) reinforcement of the earthen wall with steel plates; and (**c**) pass-through rods/bars placed every 500 mm.

To evaluate the effectiveness of the steel plate retrofit technique, two shaking table tests of reduced scale (1:4) two-story houses were performed at the Structures Laboratory of the Pontificia Universidad Javeriana. In addition, the acceleration records and the damage patterns (reinforced and unreinforced earthen houses) were compared with previous seismic tests on 1:2 and 1:1 scale specimens [8,31]. The main results show that the steel plate reinforcement significantly improves the seismic performance, demonstrating its effectiveness for two-story rammed earth houses. There is also a good agreement between the 1:4 scale test results and the larger scale tests previously conducted by the authors. This study will complement existing historic building codes with information from experimental evidence for two-story buildings, as well as lay the groundwork for new earthen standards.

2. Material Properties

In order to accurately represent a historic earthen building, rammed earth (RE) material obtained from a 120-year-old historic Colombian building that was demolished due to lack of maintenance was used to construct the specimens. The granulometry of the material was passed through a #10 sieve, taking into account the reduced scale of the specimens to be tested. This was performed to avoid failure zones due to large particles by adjusting the maximum particle size to a scale of 1:4. With this modification, the particles had a size that corresponded to the proportion of the cross section of the earthen walls built. As will be shown later, this modification of the granulometry of the material increases the compressive strength, since the new grain sizes reduce the void ratio of the rammed earth blocks and consequently increases the compactness of the material. However, as will be seen later in this document, the optimum water content and maximum dry density are very similar to the original material without granulometry modifications. The RE material was subjected to laboratory tests to determine its physical and mechanical properties and then compared with the literature. The physical properties are shown in Table 1. The granulometry, Atterberg's limits, and maximum dry density along with the optimum moisture content were evaluated according to the ASTM D422, ASTM D4318, and ASTM D698 standards, respectively [32–34]. Table 2 shows the compressive strength obtained

from compression tests on rammed earth cylinders (300 mm height and 150 mm diameter). Both tables include results from the literature of similar materials for comparison.

The data presented in Tables 1 and 2 include both the average values and the variations of the physical and mechanical properties, highlighting the distinctive attributes of the RE material used in historical constructions in the Andean region. The physical properties determined in the present research are similar to the values reported in the technical and scientific literature, but the compressive strength shows diverse average values and remarkable variability. Despite the dispersion found in the references, the average compressive strength values in the present research fall within the range of the data in Table 2. The unit weight of the RE specimens is 18.5 kN/m^3, which is in the order of magnitude presented in [31]. However, it is important to note that in some cases the current results show a difference due to the granulometry adjustment made according to the 1:4 scale of the samples. This adjustment allows a better compaction of the particles, resulting in higher values. It should be emphasized that the collapse mechanisms observed in the present research are similar to those reported for 1:1 and 1:2 scale specimens [8,31]. Finally, the steel plates used in the research were tested according to the standard ASTM A370-17 (standard test methods and definitions for mechanical testing of steel products), and had a yield stress of 194 MPa, a tensile strength of 284 MPa, and a Young's modulus of 201 GPa [35].

Table 1. Physical characteristics of RE material.

Reference	Maximum Dry Density γ_{dmax}, kN/m^3 (CoV)	Optimum Water Content w,% (CoV)	Atterberg's Limits, %			Passing Sieve, %		
			LL (CoV)	PL (CoV)	PI (CoV)	#200 (CoV)	#50 (CoV)	#4 (CoV)
Present study	17 (1%)	16 (1%)	32 (3%)	19 (3%)	12 (4%)	82 (2%)	95 (1%)	100 (1%)
[21]	17 (*)	19 (*)	32 (*)	21 (*)	11 (*)	65 ** (22%)	76 ** (22%)	86 ** (21%)
[8]	18 (7%)	15 (12%)	31 (8%)	18 (10%)	13 (23%)	69 (3%)	82 (2%)	93 (2%)
[9]	16 (0%)	17 (1%)	33 (1%)	17 (0%)	16 (3%)	77 (1%)	91 (1%)	100 (0%)
[15]	16 (1%)	17 (1%)	33 (3%)	17 (3%)	16 (0%)	78 (1%)	91 (1%)	100 (1%)

LL = Liquid Limit, *PL* = Plastic Limit, *PI* = Plasticity Index. * Not reported. ** Material data for four different buildings.

Table 2. Compressive strength.

Test	Compressive Strength, MPa
Present study	2.07 (CoV 16%)
[21]	0.55 (CoV 33%)
[2]	Range reported: 0.2~0.8
[8]	1.11 (CoV 8%)
[36]	Range for 15 references: 0.81~2.46
[9]	0.62 (CoV 12%)
[15]	1.29 (CoV not reported)

3. Reduced Scale Specimens

In the structures laboratory at the Pontificia Universidad Javeriana, two 1:4 scale RE models were constructed and tested on a biaxial MTS shaking device. One of the specimens was constructed without reinforcement, while the other was reinforced with steel plates. Both specimens were two-story, square-shaped rammed earth models. The square typology was chosen to verify the performance of the reinforcement in an earthen system that simulates the continuity of the walls. Figure 2 shows an example of a typical earthen historic Andean house and a module with this typology. The module allows for the study of the interactions between the walls and the diaphragm of the structure. In order to study the behavior of a model with four walls, instead of analyzing single walls, it was assumed that the module of the structure to be studied was detached from the building.
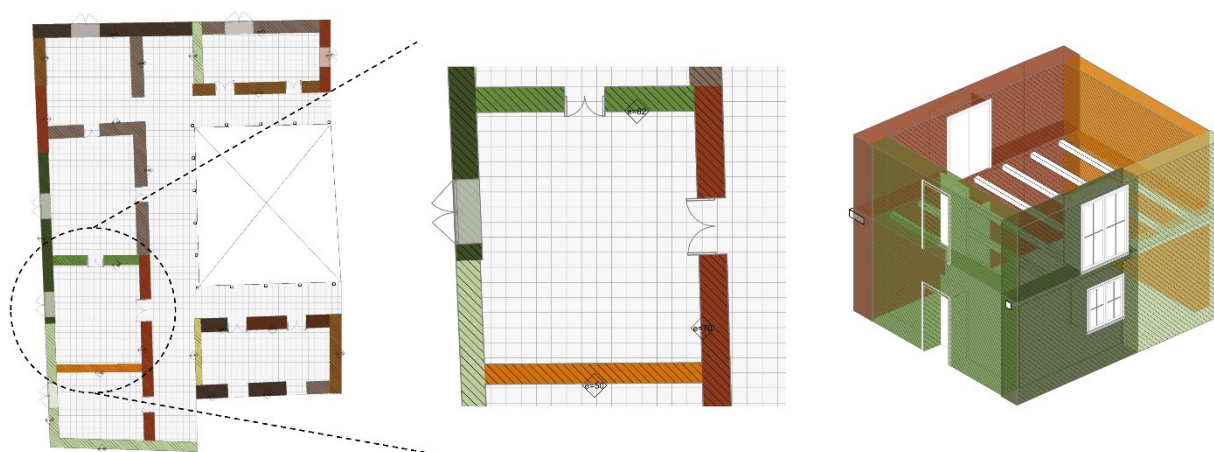

Figure 2. Typical Andean earthen house.

The choice of the 1:4 scale is determined by two main factors: First, the options for anchoring the house foundation to the shaking table given the square floor plan configuration. Second, it addresses the capacity constraints of the MTS biaxial shaking table in terms of overturning moment and maximum load (ensuring that the weight of the reinforced model does not exceed 100 kN). To the best of the authors' knowledge, there have been few examples of reduced-scale two-story earthen houses (constructions of the northern region of South America) being tested on biaxial shaking tables. In particular, this experiment is the first to subject a two-story earthen module reinforced (with steel plates), with windows and door, to a seismic-dynamic test.

The dimensions of the 1:4 models were determined according to the main characteristics of typical Andean earthen heritage constructions. The authors conducted a dimensional study focusing on walls, openings, and floors of the historic city center of Bogotá, Colombia called "La Candelaria" [30]. Figure 2 shows an example of one of the analyzed heritage houses. Through the analysis of planimetric information and field visits, it was possible to obtain statistical data on the geometric characteristics of the earthen heritage buildings. The results of the analysis showed that the average wall thickness was 640 mm and the wall height per floor was typically between 3000 mm and 3330 mm. It was also found that earthen walls usually have symmetrical openings on both floors, to accommodate windows or doors. Based on these findings, the characteristics of the reduced-scale samples were determined as explained below.

3.1. Unreinforced Model

The model constructed for the experiment was a two-story RE module, consisting of four interconnected walls with 5 windows and 1 door (Figure 3). The specimen consists of one solid wall (with no openings), two walls each with a window on both floors, and one wall with both a door and a window. This configuration is intended to accurately represent

typical architectural features (such as those shown in Figure 2), while allowing for potential differences in damage patterns and collapse mechanisms between walls with and without openings. In addition, 40 mm × 50 mm wooden scaled beams (160 mm × 200 mm in real scale) were included to represent the second floor and roof.
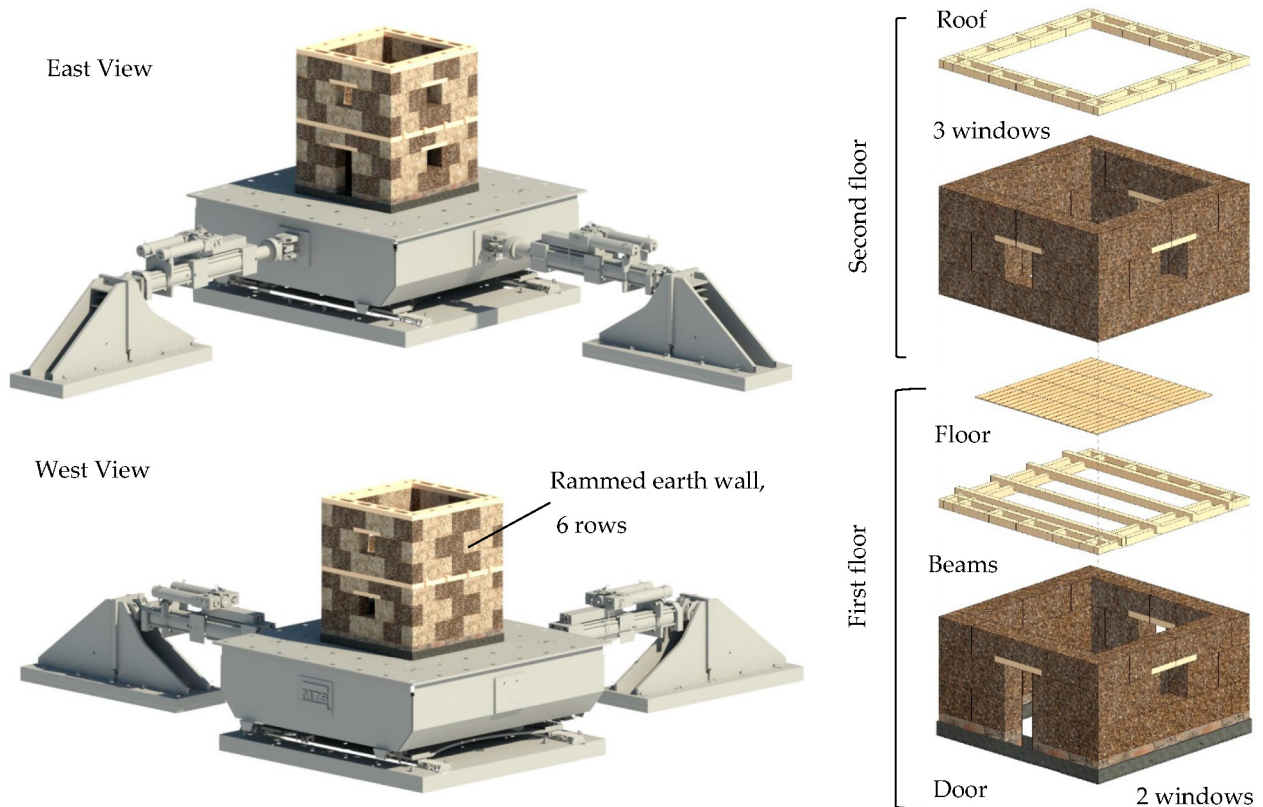

Figure 3. Two-story scaled 1:4 earthen house tested.

Wooden lintels were used over the doors and windows at the appropriate scale for the model being tested. For the 1:4 scale model, the lintels were two wooden elements, each measuring 40 mm × 80 mm (thickness × width). These dimensions in real scale correspond to a lintel made of two elements of 160 mm × 320 mm. All components and features, including construction tools, foundation stones and the rammed earth particle size, were adjusted to a scale of 1:4 and are presented in Figure 3.

The walls were constructed with compacted layers of 25 mm (100 mm at 1:1 scale), the wall thickness was 160 mm (640 mm at 1:1 scale), with a total height of 1560 mm (6240 mm at 1:1 scale). The foundation of the specimens consisted of a U-shaped steel box to simulate the boundary conditions of an earthen building. Above the foundation, an 80 mm (320 mm at 1:1 scale) height stem wall was constructed, followed by the six rows of rammed earth blocks that make up the rammed earth module. The row configuration was adopted to represent existing walls, creating interlocking connections between blocks of different rows, and ensuring structural integrity. Upon completion of construction, the soil material of the earthen blocks was allowed to dry for 30 days prior to testing.

3.2. Reinforced Module with Steel Plates

After testing the first unreinforced 1:4 scale RE model, an identical specimen was constructed using the same labor and materials used previously. After four weeks of natural drying under the controlled laboratory conditions, the second model was reinforced with confinement steel plates. This reinforcement follows the guidelines of the AIS 610-EP17 standard [19], which systematically outlines the basic requirements for the reinforcement of earthen heritage constructions in Colombia. The main objective of this reinforcement is

to significantly increase the structural stiffness and strength of the walls, both in-plane and out-of-plane, by improving their ability to resist bending and shear loads. Figure 4 shows a three-dimensional image of the two-story rammed earth model with the reinforcement system installed.
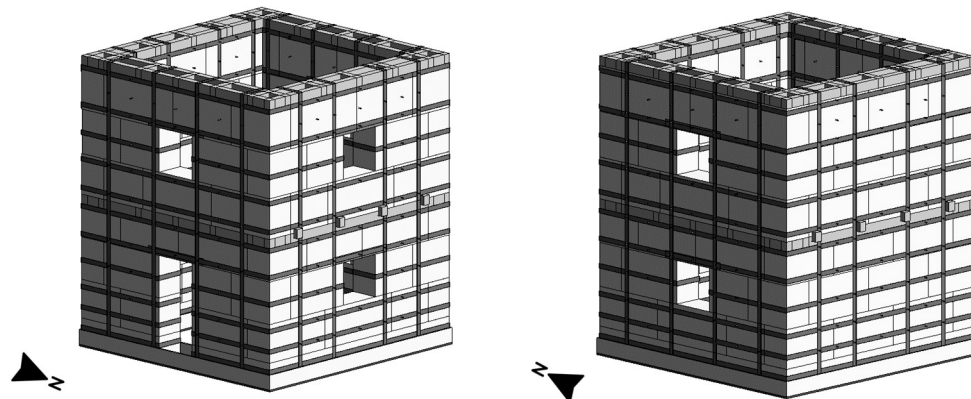

Figure 4. Reinforced 1:4 model with steel plates.

The reinforcement consists of steel plates on both sides of the walls, forming horizontal and vertical rings that confine the walls. To address the scale reduction, the steel plates were 25 mm wide and 1.6 mm thick, corresponding to a full-scale prototype in which the steel plates are 100 mm wide and 6.35 mm thick. Following the AIS 610 guidelines [19], the horizontal spacing of the reinforcement rings was limited to 250 mm (1000 mm in the full-scale prototype). An exception to this rule is the first three rings at the base, which were spaced at 125 mm (500 mm in the full-scale prototype). The vertical plates were placed 330 mm apart, a larger spacing than AIS 610 [19] (1200 mm in the prototype), based on the results of 1:2 shaking table tests performed by the authors in reference [31]. Consequently, the model had a total of 10 horizontal and 20 vertical reinforcement rings (4 vertical rings per wall). Compatibility between the steel plates and the earthen material was maintained through the use of threaded rods. In addition, these rods ensured direct contact between the plates and the surface of the walls. These rods were placed at the intersection of the horizontal and vertical rings according to AIS 610 (2017). Finally, to further strengthen the earthen house, the diaphragm of the first floor was reinforced by adding two diagonal plates that were welded to the vertical plates.

4. Reduced Scale (1:4) Biaxial Shaking Table Test

In order to extend the test results to the full-scale prototype, similarity ratios were established based on a 1:4 geometric scale neglecting gravitational forces during dynamic testing as described by the reference [37]. Previous researchers investigating the seismic performance of RE or adobe buildings have also made similar assumptions for gravitational forces, see for examples references [13,31]. Specific similarity equations for physical properties between the scale model (1:4) and the corresponding full-scale prototype are shown in Table 3. It is important to consider that the subscript "m" refers to the model, and the subscript "p" refers to the prototype.

For example, for displacement-related variables, the equation $L_m = \frac{L_p}{4}$ implies that the model dimensions are one-fourth the dimensions of the prototype. Based on the similarity ratio rules, the real acceleration records were adjusted according to Table 3 in order to control the shaking table tests by accelerations (x and y directions). It is important to emphasize that to avoid confusion, all results presented in the present research are converted with similarity equations to the prototype values (i.e., the full-scale 1:1).

Table 3. Similarity relations (gravity forces neglected) for some physical characteristics for a 1:4 scale.

Physical Variable	Similarity Factor	Model (Reduced-Scale)	Prototype (Scale 1:1)	Ratio for Scaling
Spectral displacement, or length, or displacement	1/4	L_m; Δ_m; S_{dm}	L_p; Δ_p; S_{dp}	$L_m = \frac{L_p}{4}$; $\Delta_m = \frac{\Delta_p}{4}$; $S_{dm} = \frac{S_{dp}}{4}$
Time	1/4	t_m	t_p	$t_m = \frac{t_p}{4}$
Acceleration or spectral acceleration	4	A_m; S_{am}	A_p; S_{ap}	$A_m = 4A_p$; $S_{am} = 4S_{ap}$
Frequency and angular frequency	4	f_m; ω_m	f_p; ω_p	$f_m = 4f_p$; $\omega_m = 4\omega_p$
Stress	1	σ_m	σ_p	$\sigma_m = \sigma_p$

L_m = length in the model, L_p = length in the prototype, Δ_m = displacement in the model, Δ_p = displacement in the prototype, S_{dm} = spectral displacement in the model, S_{dp} = spectral displacement in the prototype, t_m = time in the model, t_p = time in the prototype, A_m = acceleration in the model, A_p = acceleration in the prototype, S_{am} = spectral acceleration in the model, S_{ap} = spectral acceleration in the prototype, f_m = frequency in the model; f_p = frequency in the prototype, ω_m = angular frequency in the model, ω_p = angular frequency in the prototype, σ_m = stress in the model, σ_p = stress in the prototype.

4.1. Test Setup

The 3 m × 3 m shaking table was equipped with two dynamic actuators capable to generate displacements of ±250 mm in the *x* and *y* directions with a maximum acceleration of 10 g and a peak velocity limit of 1 m/s. The primary objective of these tests was to simultaneously evaluate the seismic performance of the models in both the out-of-plane and in-plane directions. Figure 5 shows the experimental setup for both models: the reinforced and the unretrofitted. The weight of the reinforced 1:4 scale model was approximately 30 kN. In addition, the model included 4.0 kN of concrete weights (at the roof) to simulate the vertical load of 5.3 kN/m per meter of the full-scale walls (gable roof) [15]. These weights were placed on a wooden platform resting on two of the walls of the rammed-earth models (Figure 5c,d). It is typical for this type of building to have gabled roofs, with two of the four walls receiving gravity loads from the roof, and this condition is simulated with the test setup. In addition, 8 kN of earth bags were used to represent the weight of the first floor and they were placed on the wooden beams of the first floor. It is important to note that the first floor has wooden beams in only one direction (Figure 3, right), so two of the four walls are loaded with the gravity loads from the floor. Based on these observations, the gravity loads are transferred to the walls with an equivalent linear load per unit length on two of the four ring beams. To anchor the earthen house to the shaking device platform, the steel box containing the foundation was anchored with 12 pre-stressed bolts. To enhance the understanding of the experimental setup, QR codes have been incorporated into Figure 5 to provide access to 360° panoramic views.

The 1:4 scale models were instrumented with a total of 18 high sensitivity piezoelectric PCB accelerometers. These miniature seismic accelerometers (weight 50 g) were ceramic and flexural with a sensitivity of 102 mV/(m/s^2), a measurement range of ±49 m/s^2, a frequency range (±3 dB) of 0.02 to 1700 Hz, a diameter of 25 mm, and a total height of 32.5 mm. Sixteen of these accelerometers were strategically placed on the walls of the earthen models, while the remaining two were placed on the shaking table. The accelerometers were placed to cover both the first and second floor walls. Each of these points was equipped with two accelerometers, oriented in both the *x* and *y* directions. These locations are shown in Figure 6 with labels from A to H.

Figure 5. (**a**) Test set up of the unreinforced model; (**b**) test set up of the reinforced model. Link for QR code 360° unreinforced model: https://pano.autodesk.com/pano.html?mono=jpgs/183016e4-f29c-4ede-95c9-bfe33a7024d3&version=2 (accessed on 22 November 2023) Link for QR code 360° reinforced model: https://pano.autodesk.com/pano.html?mono=jpgs/6d32568d-f123-4ce6-9d34-4675c3ce6dc1&version=2 (accessed on 22 November 2023) (**c**) Photograph of the experimental setup of the unreinforced model and (**d**) photograph of the experimental setup of the reinforced model.
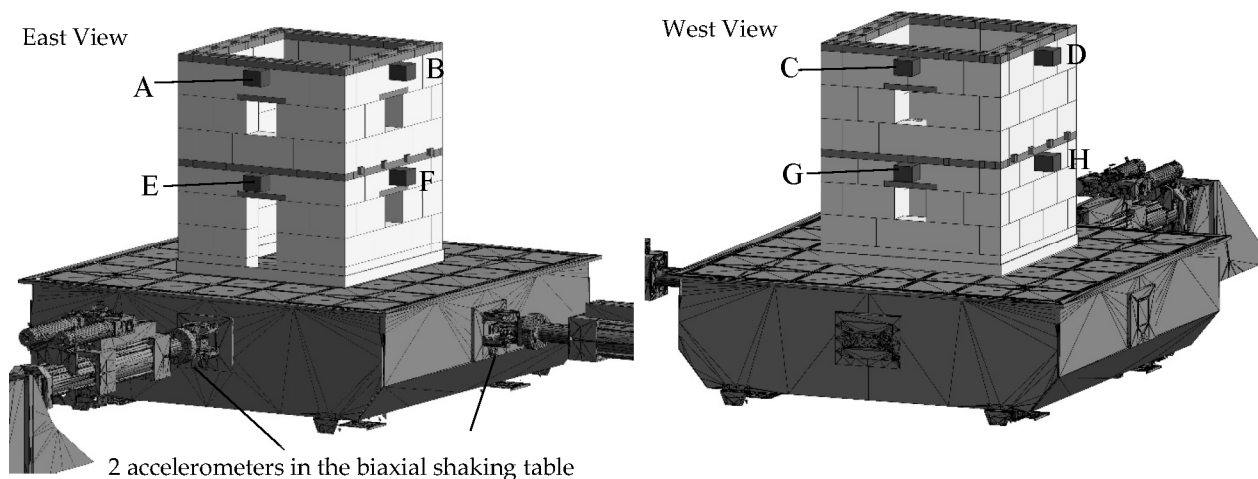
Figure 6. Location of accelerometers A to H.

4.2. Test Protocol

The loading protocol for this test was based on a seismic disaggregation analysis following the procedure described by [8,31,38]. The analysis covers periods in the range 0.3 s to 1.0 s. For the seismic simulation, specific ground motions corresponding to return periods of 2500, 475, 225, and 31 years were used. These return periods are related to 2%, 10%, 20%, and 80% exceedance probabilities in 50-years, respectively. Table 4 presents the *PGA* values for the prototype (full scale) and for the scaled models.

Table 4. Protocol for the shaking table tests. Adapted from [8,31,38].

Step	Input Record (Station Name)	Exc. Prob. in 50 Years	M_W (Dist.)	PGA (y-Direction)/g		PGA (x-Direction)/g	
				Prototype	Model	Prototype	Model
1	Quetame 2008 (Bogota–Vitelma)	80%	5.9 (55 km)	0.14	0.56	0.11	0.44
2	Loma Prieta (scaled), 1989 San Francisco Int. Airport	20%	6.9 (59 km)	0.38	1.52	0.29	1.16
3	Loma Prieta (scaled), 1989 San Francisco Int. Airport	10%	6.9 (59 km)	0.43	1.72	0.34	1.36
4	Loma Prieta (scaled), 1989 San Francisco Int. Airport	2%	6.9 (59 km)	0.53	2.12	0.39	1.56
5	Loma Prieta (scaled), 1989 San Francisco Int. Airport	*	6.9 (59 km)	0.76	3.04	0.55	2.22
6	Loma Prieta (scaled), 1989 San Francisco Int. Airport	**	6.9 (59 km)	1.02	4.08	0.78	3.12

* This ground movement corresponds to 150% the record with a probability of exceedance of 2% in 50 years,
** This ground movement corresponds to 200% the record with a probability of exceedance of 2% in 50 years.

5. Crack and Damage Patterns

The damage progression of the unreinforced and reinforced houses after the seismic motions is shown in Figure 7. The unreinforced specimen partially resisted earthquake phases with PGA_y of 0.14 g, 0.38 g, 0.43 g, and 0.53 g, and showed irreparable damage and partial collapse during the event with $PGA_y = 0.53$ g followed by a complete collapse during the earthquake with $PGA_y = 0.76$ g. In contrast, the reinforced house withstood the entire sequence of ground motions up to an earthquake with $PGA_y = 1.02$ g (a total of six ground motions), with damage in some points of the stone stem wall, but with little damage in the rammed earth walls. It is noteworthy that in the reinforced house, the diaphragm works adequately to transfer the seismic forces to the reinforced walls, providing structural integrity to the system.

The first cracks in the unreinforced model appeared in the masonry joints between the rammed earth blocks and at some stress concentration points near the wall openings. These cracks were more pronounced for $PGA_y = 0.53$ g. Diagonal cracks also appeared in the lower part of the walls, even passing through entire rammed earth blocks. At a PGA of 0.53 g, the size of pre-existing cracks increased and horizontal cracks also appeared. Then, at 0.76 g, new horizontal, vertical, and diagonal cracks were noticeable and began to affect the stability of the model. A diagonal crack in one of the corners of the wall without openings, which crossed both the joint between the blocks and the blocks themselves, stands out. A dislocation of the rammed earth blocks can also be seen, as reported in references such as [21,31]. This phenomenon is critical in the corner areas because the loss of material from the blocks inevitably destabilizes the structural system, and it is precisely this condition that generates the catastrophic failure of the unreinforced model for the next load step.

In contrast, the reinforced model had a lower level of cracking and damage for all the PGA of the loading protocol. As for the unreinforced model, the first cracks appeared for the motion with $PGA_y = 0.43$ g. These cracks were vertical and several horizontal cracks in the lower zone of the second-story wall. For the motion with $PGA_y = 0.53$ g, the same cracks from the previous motion increased in size, indicating flexural behavior. It is important to note that several of these cracks correspond to the factory joints of the different rammed earth blocks. It should also be noted that there were no oblique cracks typical of shear failure. Finally, for the last two shaking table motions, corresponding to PGA of

0.76 g and 1.02 g, the damage was mainly concentrated at the base of the first floor wall. The behavior and cracking pattern presented above had a predominance of vertical and horizontal cracks related to bending effects rather than diagonal shear cracks reported in other references for earthen walls subjected to in-plane loading. Furthermore, this pattern is consistent with the results reported in references [8,31] for the same seismic motions. Moreover, these last two studies were carried out on models of larger dimensions (real scale 1:1 in reference [8] and scale 1:2 in reference [31]) with materials and construction typology similar to the one tested in the present research. In particular, the damage concentration in the lower part of the reinforced model was observed in reference [31] for the same seismic motions but on 1:2 scale models of C-shaped walls.
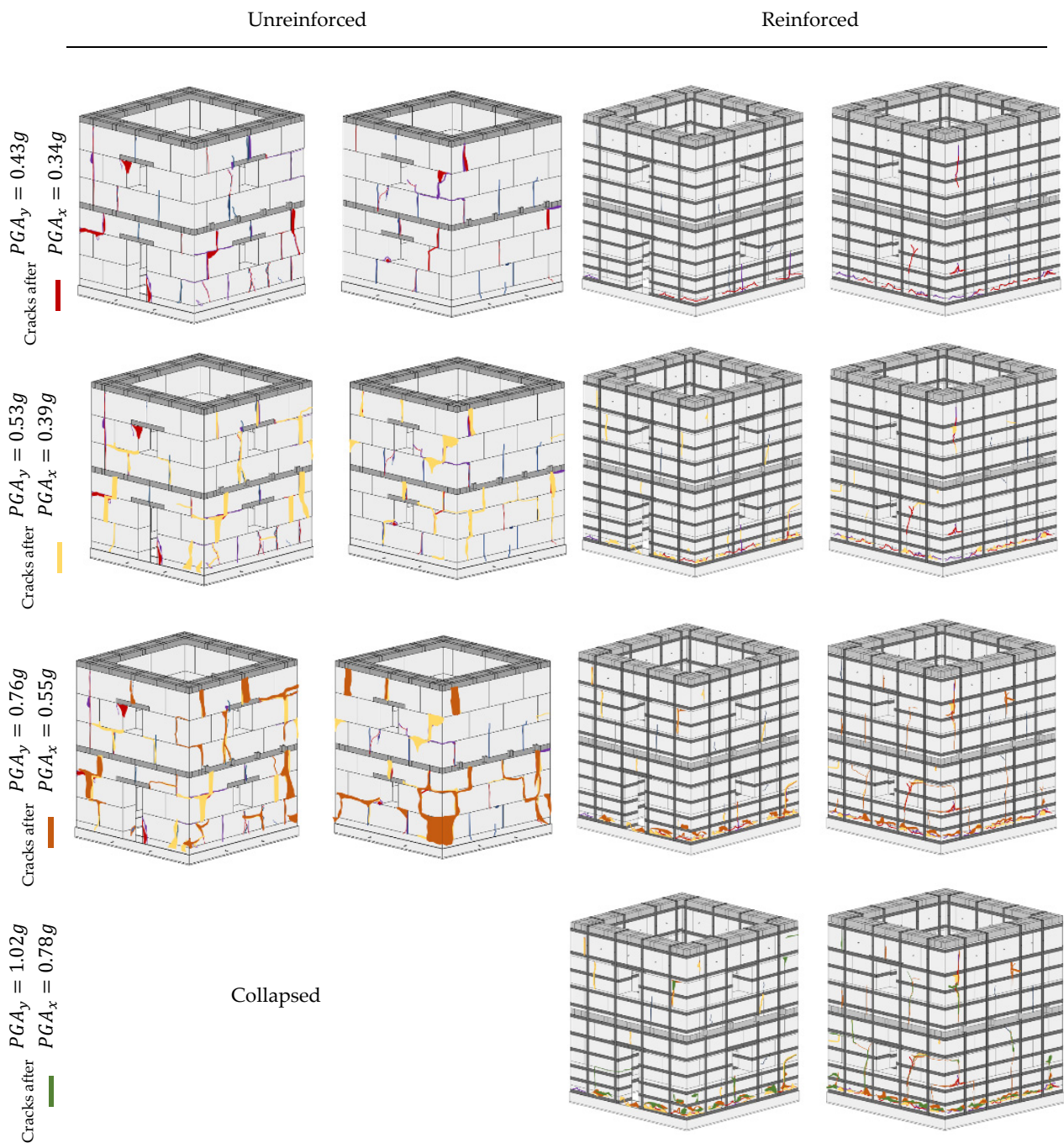
Figure 7. Damage patterns of unreinforced (**left**) and reinforced specimens (**right**).

Figure 7 also shows that the second floor of the models had fewer cracks than the first floor in both models. However, the damage in the unreinforced model was extensive, with vertical and diagonal cracks in the walls originating at the joints of the rammed earth blocks, due to block detachment and corner earth separation in the structural assembly. In contrast, the reinforced model showed localized and repairable damage manifested as limited vertical or diagonal cracking. It is important to emphasize that, the damage at the base in the reinforced model, particularly at the rock-wall junction, was significantly more pronounced compared to the unreinforced structure. At the same time, the buckling of the plates induced damage at the stem wall for a $PGA_y = 0.53$ g. This buckling was also observed in reference [31], which tested a two-story RE wall, while it was not evident in the test of the one-story earthen walls in reference [8]. Therefore, this damage pattern can be attributed to the additional overturning moment at the base of the walls due to the mass of the second-story. In conclusion, the test results indicate that steel plates prevent wall failure, delay cracking, and improve the displacement capacity of the model.

In contrast to what was reported in references [8,31], the modules tested in the actual research (both reinforced and unreinforced) withstood an additional increase in the loading protocol defined in Table 4. The authors hypothesize that this better behavior may be due to the redundancy of the four-wall modules tested in the present research compared to the C-shaped wall (from reference [31]) and the L-shaped wall from reference [8]. Having four walls with two diaphragms may reduce the possibility of dislocation of the RE blocks, which was one of the failure mechanisms reported in both references.

6. Acceleration Records

Figure 8 shows an example of the acceleration records at one of the points of the second floor (point D) for both the unreinforced and the reinforced prototype. In order to facilitate the interpretation of the measurements made, all the results presented refer to the prototype (scale 1:1). For this purpose, the experimental results have been adjusted according to the similarity laws presented in Table 3. For each data set, the peak acceleration value is highlighted.

Accelerations in two mutually perpendicular directions (x and y directions) were recorded at each point, but only the movements for the y-direction (critical direction) are shown in Figure 8. For all the data sets analyzed, it was found that the peak accelerations at all the points of the reinforced prototype are higher than those of the unreinforced prototype. In addition, the reinforced specimen withstood all six intensities of ground motions, while the unreinforced specimen showed partial collapse for $PGA_x = 0.55$ g and $PGA_y = 0.76$ g. The reinforced prototype with steel plates experienced a maximum acceleration of 1.24 g at point D for the maximum $PGA_y = 1.02$ g.

Figures 9 and 10 show the profile of the maximum accelerations for each of the ground motions of the shake table protocol. The value reported for each floor is the average of the four accelerometers installed at each level of the specimen (reinforced and unreinforced). The selected motions had a direction of greater intensity, which is the y-direction for the present research. For the unreinforced prototype (Figure 10), the results are shown only for the first four intensity levels because the unreinforced specimen was severely damaged after the ground movement with $PGA_y = 0.53$ g. Based on the results, it can be concluded that the acceleration of the upper floors was always higher than that of the lower floor in both x and y directions and this distribution indicates a clear first mode response. The maximum acceleration of the unreinforced prototype was 0.76 g (for $PGA_y = 0.53$ g) in the y-direction. For the same earthquake motion, but in the x direction ($PGA_x = 0.39$ g), the average maximum acceleration of the second floor was 0.55 g. According to the results of the acceleration profiles of the reinforced prototype, a maximum acceleration of 1.22 g and 0.92 g was reached in the y and x directions, respectively. These maximum accelerations were reached for the last movement at the base of the loading protocol.
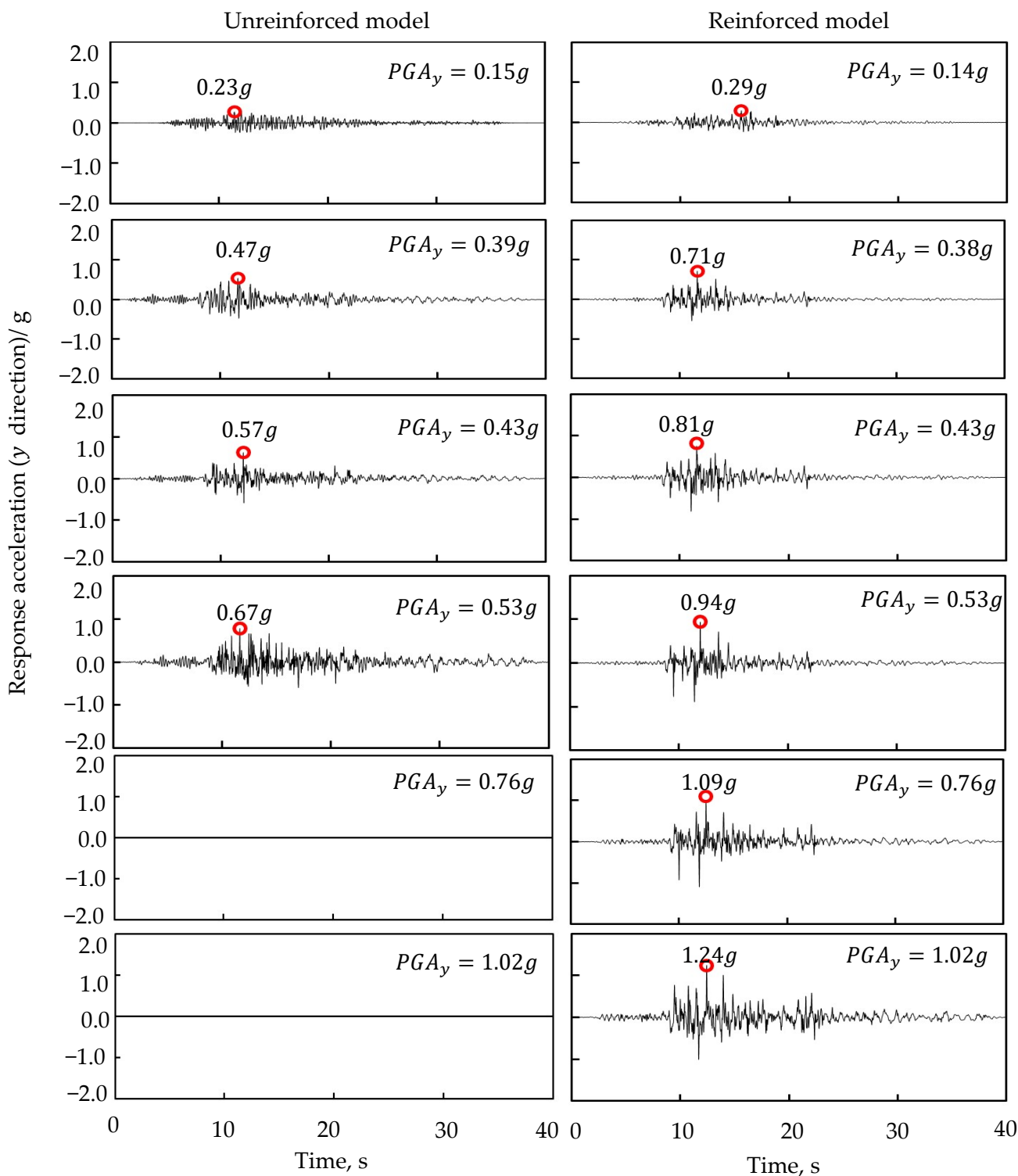
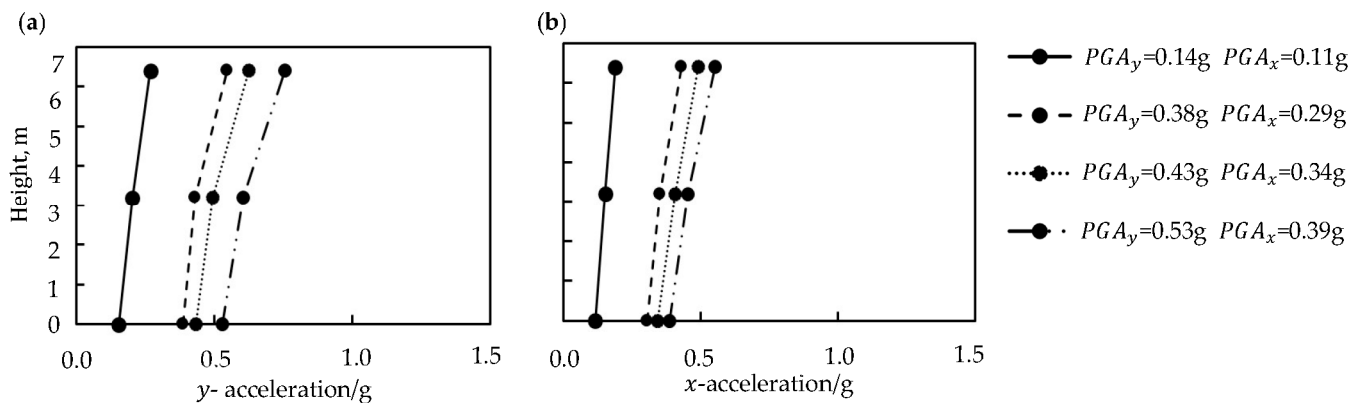**Figure 8.** Acceleration in *y*-direction recorded in point D.

Figure 9. Unreinforced prototype: (**a**) *y*-acceleration profile, (**b**) *x*-acceleration profile.
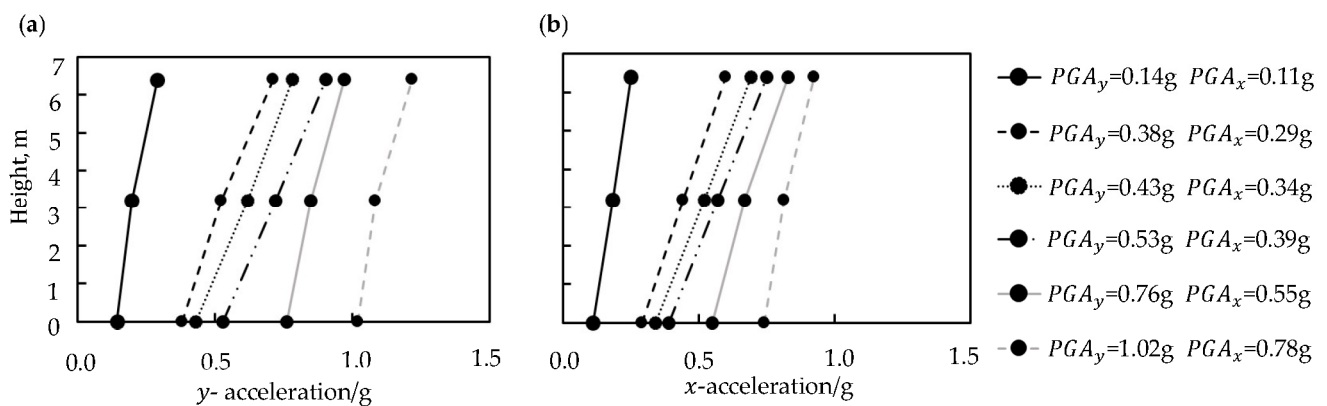

Figure 10. Reinforced prototype: (**a**) *y*-acceleration profile, (**b**) *x*-acceleration profile.

Despite these high levels of *PGA* and accelerations at the first and second floors, the reinforced specimen showed little damage (as shown in Figure 8) and the steel plates confined the rammed earth blocks and absorbed the flexural tensile stresses, reducing the damage of the specimen. At these maximum acceleration levels, the second floor of the reinforced specimen showed less damage and cracking than the first floor. As reported by [31], the steel plates confining the RE blocks reduce the possibility of dislocation. Based on the experimental results, the reinforcement system reduces the fragility of the rammed earth walls and gives the structural system an inelastic displacement capacity.

7. Comparison of Accelerations between Scale Reinforced Models

Table 5 presents a comparison of the maximum accelerations determined for the present study (1:4 scale two-story reinforced earthen module) with the maximum accelerations measured in two previous tests conducted by the authors and presented in references [8,31]. All three specimens tested used soil from demolished houses in the Andean region of northern South America, and the three models were constructed using the rammed earth technique. For comparison purposes, Figure 11 shows the schemes and the main characteristics of the three models retrofitted with steel plates, which are compared in terms of maximum accelerations. This figure shows relevant information such as the scale, the dimensions of the prototype they represent, the number of stories and the initial period (elastic) of the full-scale prototype. These periods were determined from the experimental results for all the three specimens based on the analysis of the recorded acceleration data. It is important to note that the fundamental elastic natural periods of the full-scale prototypes representing the three buildings tested are of the same order of magnitude, about 0.3 s, so their dynamic response could be comparable. The comparison of maximum accelerations is shown in Table 5 for the out-of-plane direction for five ground motion intensities. Table 5

includes data on the accelerations of a one-story steel plate reinforced RE wall, whose shaking table results (uniaxial ground motions) are reported in reference [8]. In addition, Table 5 shows the out-of-plane results for the two-story C-shaped wall of the reference [31]. The current research analyzes a four-wall module with openings, while the references [8,31] tested walls without doors or windows. Both two-story scale models were built with RE walls and included a floor system with crown beam and load-bearing wood beams.

Table 5. Comparison of the average out-of-plane accelerations (first and second floor) of a 1:1 scale prototype estimated from the data of the present study and values interpolated from graphs of references [8,31].

PGA out-of-Plane, g	Level	Prototype Acceleration, g		
		Values Interpolated from Graphs of Reference [31]	**Present Study**	**Values Interpolated from Graphs of Reference [8]**
0.76	Floor 2	1.33	1.07	1.65
	Floor 1	1.07	0.93	----
0.53	Floor 2	0.92	0.90	1.15
	Floor 1	0.68	0.72	----
0.43	Floor 2	0.76	0.78	0.83
	Floor 1	0.56	0.62	----
0.38	Floor 2	0.62	0.71	0.83
	Floor 1	0.47	0.52	----
0.14	Floor 2	0.25	0.29	0.35
	Floor 1	0.19	0.21	----
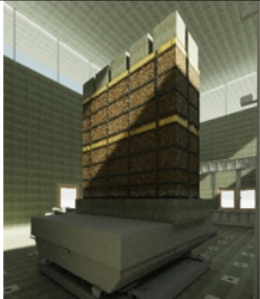
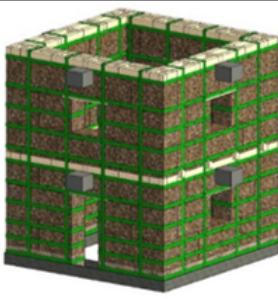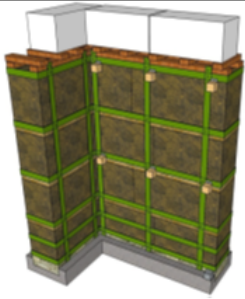| Model			
Scale	1:2	1:4	1:1
Description	Individual rammed-earth wall	Four rammed earth walls	Individual rammed-earth wall
Dimensions of real scale prototype (Length x height)	5900 m x 6300 m	5400 m x 6240 m	3000 m x 3500 m
Floors	Two levels	Two levels	One level
Initial period (s) of the prototype (full scale)	0.34	0.27	0.25
Reference	Adapted from Ruiz, et al., 2023	Current study	Adapted from Reyes, et al. 2020

Figure 11. Main characteristics of the three wall models being compared [8,31].

The three reinforced (with steel plates) earthen models (the present study, reference [8,31]) were subjected to ground motions with the same loading protocol defined in Table 4, although in each case adapted to the scale of the test according to the similarity rules presented in Table 3. The model from reference [8] was tested unidirectional with the ground motions in the *y*-direction of Table 4 while the other two models were tested with a biaxial protocol. Considering the data in Table 5, although the 1:1 scale model tested in reference [8] has only one floor, the results for the maximum accelerations recorded are in the same order of

magnitude as the acceleration values of the second floor of reference [31] and the present study. In addition, the experimental data suggest that the results of the accelerations of the equivalent prototypes of each test (which had natural periods close to 0.3) are in the same order of magnitude for all the loading protocol (five intensities motions). The above facts suggest that RE models following the guidelines of reference [37] allow to reasonably estimate the maximum accelerations of large prototypes. However, this is generally true only if the spatial model has external (outer or perimeter) walls of higher stiffness and also floors of a lightweight wood structure. In this case, the behavior of the building on a macro scale can be inferred from tests on smaller models, but only if the natural periods are similar. Differences could be found between the model and the prototype if there is asymmetric behavior (due to geometry or internal walls) and, as a result, other types of failure modes are likely to occur.

8. Conclusions

The steel plate reinforcement system reduces the cracking and the possibility of dislocation of the earthen blocks that conform RE walls. Additionally, the retrofitting system provides the earthen buildings with an energy dissipation capacity, good behavior in the inelastic range, and confinement of the earthen constructions.

The failure mechanism of the unreinforced earth model subjected to the seismic shaking table test is the appearance of flexural and shear cracks that induce the dislocation of the earth blocks and, consequently, the instability and collapse of the walls. According to the experimental results, the cracks appear to be critical at $PGA_y = 0.53$ g and $PGA_x = 0.39$ g.

Effectively, the steel plate reinforcement system provides continuity, connection, and confinement to the rammed earth walls, and as a consequence, the reinforced model withstood the entire load protocol up to peak ground acceleration values of $PGA_y = 1.02$ g and $PGA_x = 0.78$ g. For these PGA values, the maximum average roof acceleration was 1.22 g with no signs of structural collapse. After the loading protocol, the reinforced module presented repairable damage in the zone of the stem wall. This evidence confirms that the steel plate reinforcement system provides resilience to RE buildings even during high intensity earthquakes.

Comparing the results of the 1:4 scale tests of the present research with the 1:2 and 1:1 scale tests previously conducted by the authors, the accelerations of the prototypes are in the same order of magnitude. This means that it is possible to estimate the maximum accelerations of RE building prototypes using reasonably small-scale models.

References

1. Xie, L. Architectural energetics for rammed-earth compaction in the context of Neolithic to early Bronze Age urban sites in Middle Yellow River Valley, China. *J. Archaeol. Sci.* **2021**, *126*, 105303. [CrossRef]
2. Ruiz, D.M.; Lopez, C.; Rivera, J.C. Propuesta de normativa para la rehabilitación sísmica de edificaciones patrimoniales [Proposed regulations for seismic rehabilitation of earthen heritage buildings]. Apuntes: Revista de Estudios Sobre Patrimonio Cultural. *J. Cult. Herit. Stud.* **2012**, *25*, 2.
3. Gandreau, D.; Delboy, L. UNESCO-CRAterre-ENSAG. World Heritage. Inventory of Earthen Architecture. 2012. Available online: https://whc.unesco.org/document/116577 (accessed on 22 November 2023).
4. Ruiz, D.M.; López, C.; Unigarro, S.; Domínguez, M. Seismic Rehabilitation of Sixteenth-and Seventeenth-Century RE–Built Churches in the Andean Highlands: Field and Laboratory Study. *J. Perform. Constr. Facil.* **2015**, *29*, 04014144. [CrossRef]
5. Hall, M.; Lindsay, R.; Krayenhoff, M. Modern Earth Buildings: Materials, Engineering, Constructions and Applications. Modern earth building codes, standards and normative development. In *Modern Earth Buildings*; Woodhead Publishing Series in Energy; Schroeder, H., Ed.; Woodhead Publishing: Sawston, UK, 2012; Chapter 4.
6. Blondet, M.; Villa-Garcia, G.; Brzev, S.; Rubiños, Á. Earthquake-resistant construction of adobe buildings: A tutorial, EERI/IAEE World Hous. *Encyclopedia* **2011**, *56*, 13–21.
7. D'Ayala, D.; Eeri, M.; Benzoni, G. Historic and Traditional Structures during the 2010 Chile Earthquake: Observations, Codes, and Conservation Strategies. *Earthq. Spectra.* **2012**, *28*, 425–451. [CrossRef]
8. Reyes, J.C.; Rincon, R.; Yamin, L.E.; Correal, J.F.; Martinez, J.G.; Sandoval, J.D.; Gonzalez, C.D.; Angel, C.C. Seismic retrofitting of existing earthen structures using steel plates. *Constr. Build. Mater.* **2020**, *230*, 117039. [CrossRef]
9. Ruiz, D.M.; Reyes, J.C.; Bran, C.; Restrepo, M.; Alvarado, Y.A.; Barrera, N.; Suesca, D. Flexural behavior of rammed earth components reinforced with steel plates based on experimental, numerical, and analytical modeling. *Constr. Build. Mater.* **2022**, *320*, 126231. [CrossRef]
10. Bui, T.-L.; Bui, T.-T.; Bui, Q.-B.; Nguyen, X.-H.; Limam, A. Out-of-plane behavior of rammed earth walls under seismic loading: Finite element simulation. *Structures* **2020**, *24*, 191–208. [CrossRef]
11. Tavares, A.; Costa, A.; Varum, H. Common pathologies in composite adobe and reinforced concrete constructions. *J. Perform. Constr. Facil.* **2012**, *26*, 389–401. [CrossRef]
12. Varum, H.; Silviera, D.; Figeiredo, C.; Costa, A. Structural Behaviour and Retrofitting of Adobe Masonry Buildings, Structural Rehabilitation of Old Buildings. *Build. Pathol. Rehabil.* **2014**, *2*, 37–75. [CrossRef]
13. Tarque, N.; Blondet, M.; Vargas-Neumann, J.; Yallico-Luque, R. Rope mesh as a seismic reinforcement for two-storey adobe buildings. *Bull. Earthq. Eng.* **2022**, *20*, 3863–3888. [CrossRef]
14. Rincon, R.; Reyes, J.C.; Carrillo, J.; Clavijo-Tocasuchyl, A. Empirical fragility assessment of adobe and rammed earth walls subjected to seismic actions. *Earthq. Eng. Struct. Dyn.* **2022**, *51*, 1133–1157. [CrossRef]
15. Ruiz, D.M.; Barrera, N.; Reyes, J.C.; Restrepo, M.; Alvarado, Y.A.; Lozada, M.; Vacca, H.A. Strengthening of historical earthen constructions with steel plates: Full-scale test of a two-story wall subjected to in-plane lateral load. *Constr. Build. Mater.* **2023**, *363*, 129877. [CrossRef]
16. Norma E.080: Diseño y construcción con tierra reforzada; El Peruano, Spanish, Lima, Peru. 2017. Available online: https://procurement-notices.undp.org/view_file.cfm?doc_id=109376 (accessed on 22 September 2023).
17. Standards Australia. *The Australian Earth Building Handbook*; Standards Australia: Sydney, Australia, 2002.
18. Lhem, D. Lehmbau Regeln: Begriffe Baustoffe Bauteile. In *Earth Building Rules: Terms Building Materials Building Components*, 3rd revised ed.; Vieweg+Teubner Verlag: Berlin/Heidelberg, Germany, 2009.
19. *Norma AIS-610-EP-2017*; Evaluación e Intervención De Edificaciones Patrimoniales de uno y dos Pisos de Adobe y Tapia Pisada [Evaluation and Intervention of one- and Two-story Adobe and Rammed-Earth Heritage Building]. AIS-Asociación Colombiana de Ingeniería Sísmica: Bogota, Colombia, 2017.
20. Bossio, S.; Blondet, M.; Rihal, S. Seismic behavior and shaking direction influence on adobe wall structures reinforced with geogrid. *Earthq. Spectra.* **2013**, *29*, 59–84. [CrossRef]
21. Yamín, L.E.; Phillips, C.; Reyes, J.C.; Ruiz, D.M. Estudios de vulnerabilidad sísmica, rehabilitación y refuerzo de casas en adobe y tapia pisada [Seismic vulnerability studies, rehabilitation and reinforcement of adobe and rammed earth houses]. *Apunt. Rev. Estudios Sobre Patrim. Cult.* **2007**, *20*, 286–303.
22. Blondet, M.; Torrealva, D.; Ginocchio, F.; Vargas, J.; Velásquez, J. Seismic reinforcement of adobe houses using external polymer mesh, in: 8th US Natl. *Conf. Earthq. Eng.* **2006**, *2006*, 4223–4232.
23. Charleson, A.; Blondet, M. Seismic reinforcement for adobe houses with straps from used car tires. *Earthq. Spectra.* **2012**, *28*, 511–530. [CrossRef]
24. Liu, K.; Wanga, M.; Wang, Y. Seismic retrofitting of rural RE buildings using externally bonded fibers. *Constr. Build. Mater.* **2015**, *100*, 91–101. [CrossRef]
25. Miccoli, L.; Müller, U.; Pospíšil, S. RE walls strengthened with polyester fabric strips: Experimental analysis under in-plane cyclic loading. *Constr. Build. Mater.* **2017**, *149*, 29–36. [CrossRef]
26. Hamilton, H.R.; McBride, J.; Grill, J. Cyclic testing of RE walls containing post-tensioned reinforcement. *Earthq. Spectra.* **2006**, *22*, 937–959. [CrossRef]

27.　Cassese, P.; Balestrieri, C.; Fenu, L.; Asprone, D.; Parisi, F. In-plane shear behaviour of adobe masonry wallets strengthened with textile reinforced mortar. *Constr. Build. Mater.* **2021**, *306*, 124832. [CrossRef]

28.　López, C.; Ruiz, D.M.; Jerez, S.; Aguilar, S.; Torres, J.; Alvarado, Y.A. Seismic behavior of RE buildings reinforced with wood elements and an upper concrete beam. *Inf. Constr.* **2020**, *72*, e347. [CrossRef]

29.　Gómez, V.; López, C.; Ruiz, D. Seismic rehabilitation of rammed-earth heritage buildings: Study case of doctrinal church. *Inf. Constr.* **2016**, *68*, e140. [CrossRef]

30.　Ruiz, D.M.; Barrera, N.; Reyes, J.C.; López, C.; Restrepo, M. An approach to Colombian Andean earthen architecture in urban environments: A case study of Bogotá Historic Centre. *J. Archit. Conserv.* **2022**, *29*, 168–192. [CrossRef]

31.　Ruiz, D.M.; Barrera, N.; Reyes, J.C.; Alvarado, Y.A.; Villalba-Morales, J.D.; Gómez, I.D.; Vacca, H.A.; Carrasco, D. Bi-axial shaking table tests to evaluate the seismic performance of two-story rammed-earth walls retrofitted with steel plates. *Bull. Earthq. Eng.* **2023**, *21*, 6393–6422. [CrossRef]

32.　*ASTM D422*; Standard Test Method for Particle-Size Analysis of Soils. ASTM-American Society for Testing and Materials: West Conshohocken, PA, USA, 2007.

33.　*ASTM D4318*; Standard Test Methods for Liquid Limit, Plastic Limit, and Plasticity Index of Soils. ASTM-American Society for Testing and Materials: West Conshohocken, PA, USA, 2017.

34.　*ASTM D698*; Standard Test Methods for Laboratory Compaction Characteristics of Soil Using Standard Effort. ASTM-American Society for Testing and Materials: West Conshohocken, PA, USA, 2021.

35.　*ASTM A370-17*; Standard Test Methods and Definitions for Mechanical Testing of Steel Products. ASTM-American Society for Testing and Materials: West Conshohocken, PA, USA, 2017.

36.　Avila, F.; Puertas, E.; Gallego, R. Characterization of the mechanical and physical properties of unstabilized RE: A review. *Constr. Build. Mater.* **2020**, *270*, 121435. [CrossRef]

37.　Harris, H.; Sabnis, G. *Structural Modeling and Experimental Techniques*, 1st ed.; CRC Press: Boca Raton, FL, USA, 1999.

38.　Reyes, J.C.; Galvis, F.; Yamín, L.E.; Gonzalez, C.; Sandoval, J.D.; Heresi, P. Out-of-plane shaking table tests of full-scale historic adobe corner walls retrofitted with timber elements. *Earthq. Eng. Struct. Dyn.* **2019**, *48*, 888–909. [CrossRef]